Ratcheting of Granular Polymer in Response to a Spatial Symmetry Breaking

Y.-C. Lin, C.-C. Chang, C.-W. Peng†, W.-T. Juan* and J.-C. Tsai*
Institute of Physics, Academia Sinica, Taipei, TAIWAN 11529

(Dated: 2012.04.24.ppw-2012Letter-jc12.009c05.tex)

We study a short chain of loosely connected millimeter-sized solid spheres in response to vertical vibrations whose intensity has a gradient that is perpendicular to the movements of the substrate. The behaviours of the chain exhibit a generic dependence on its location showing a crossover, from steady crawling towards the decrease of vibration, to rapid unstable movements as the excitation intensifies. Our time-resolved three-dimensional particle tracking confirms that this crossover can be identified with two qualitatively different modes of ratcheting. The critical angle for uphill climbing in the presence of a finite tilt exhibits a strong correlation to the magnitude of the gradient. The fact that the rate of ratcheting goes far beyond the numerical assessment based on purely stochastic kicks operated at their theoretical upper limit suggests that the observed motion results from correlated movements along this macroscopic polymer in response to the small spatial asymmetry.

Ratcheting of macroscopic objects has sparked many inspiring discussions in the research community. Among recent examples, Kudrolli and co-workers [1] have demonstrated that a rigid dimer on a vibrating table can spontaneously choose from one of the multiple modes that are simultaneously available, exhibiting a stochastically determined ratcheting. For a deformable object such as a liquid drop vibrated in gravity, series of experimental and theoretical works [2, 3] have investigated how the tilt angle of the substrate, or the phase difference between two coupled components of vibrations, would determine the induced periodic but time-irreversible deformation of the drop and in turn the ratcheting. Other evidence and theories exist for the ratcheting of asymmetrical object [4], and for the rotation and swirling of objects with chirality [5], both in the context of a uniform excitation. But can we predict the response of a symmetrical object to vibrations with a spatial bias in the intensity, in analogy to the temperature gradient in nature? It seems that, despite the long tradition of studies across disciplines on thermophoresis (biased molecular diffusion) and thermotaxis (migration of micro-organisms), straightforward predictions for this macroscopic counterpart are still unreported.

We are, in particular, interested in the response of deformable objects in a gradient field. "Granular polymer" offers such example, which refers to a chain of loosely constrained solid spheres in many previous works[6–10]. Easily found in daily lives, these chains have been well characterized by researchers. State-of-art internal imaging has been applied to obtain in-depth knowledge on the packing and responses of the bulk in various contexts. [9, 10] On a vibration table, the analogies of granular chains to molecular polymers have been widely explored [6–8].

We build a shaker that allows us to impose sinusoidal vibrations with an intensity linearly distributed along the x-axis shown as in Fig. 1. The origin $x = 0$ marks the location of a frictionless bearing where the vibration vanishes. The granular polymer being used is a chain of eight identical steel spheres that are free to move except the maximal spacing between adjacent ones are constrained – see Ref. [9] for its tomography. The entire chain is about 1/20 the length of the substrate. Gravitational acceleration g goes in the direction of -z, while the chain is partially constrained in the y-direction by either type of the track as shown by the cross-sectional graph. We are also able to impose an additional tilt θ_0 by adjusting the height difference between the bearing and the spring suspension, so that the effective force can be assessed. Special cares are taken to ensure that the base is secure, that the substrate is sufficiently rigid, and that we use a non-contact electromagnetic driving to avoid undesired horizontal coupling such that the oscillation at every point is indeed a simple harmonic motion vertically, as we have verified by measuring both the wave form of the acceleration and its linearity with x.

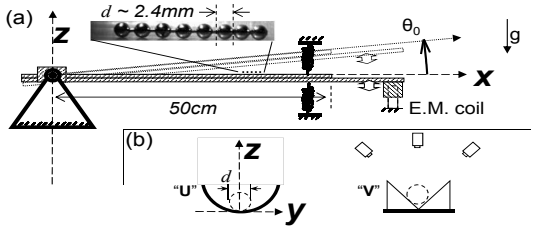

FIG. 1. Set up of the linear shaker with two types of track, and the definition of our spatial coordinates.

For the convenience of analyses, two dimensionless functions of space are defined: the peak intensity of acceleration $\Gamma(x)$ in units of g, and the dimensionless gradient $\eta(x) \equiv \ell \cdot \kappa(x)$, in which $\kappa(x) \equiv \frac{grad\,\Gamma}{\Gamma} = 1/x$. The length scale ℓ depends on the granular polymer. The typical driving frequency ranges from 15Hz to 25Hz, and we use the value $VS \equiv \Gamma|_{x=25cm}$ to specify the overall vibration strength for each experiment.

We show in Fig. 2(a) a generic collection of data. Center-of-mass positions of the chain are plotted against

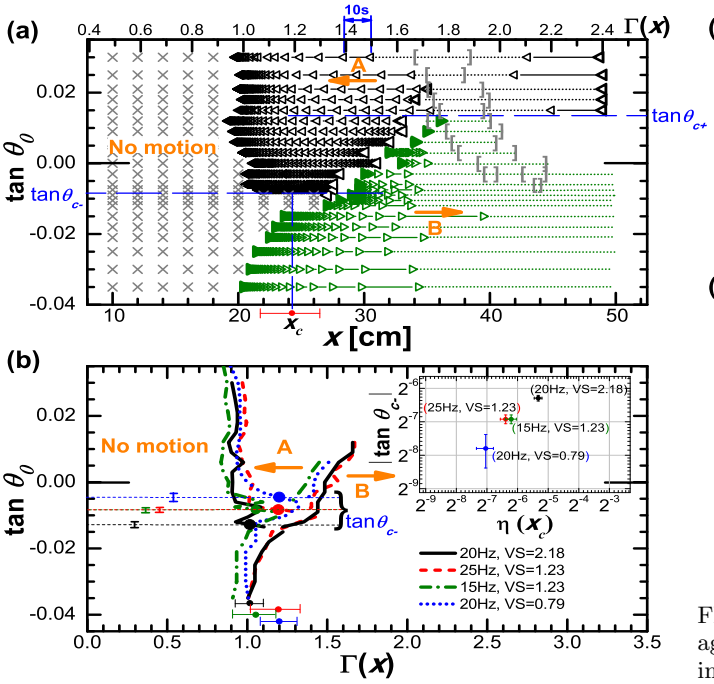

FIG. 2. Ratcheting motion at different tilt angles **(a)** Time-elapsed plots of the center of mass of the chain in a typical condition (25Hz, VS=1.23, V-track). The orientation of triangles indicates the direction of ratcheting and its divide. The initial positions of these experiments are indicated by an enlarged symbol. The brackets mark the intervals where the chain is identified with significant back-and-forth movements (over 0.4cm in amplitudes). **(b)** Boundaries collected from four groups of data with different frequencies and vibration strengths, plotted against the local intensity Γ. **Inset**: the critical slope $|\tan\theta_{c-}|$ versus the dimensionless gradient η, with the characteristic length ℓ therein set as $2.6mm$ (the typical spacing between contacts with the substrate.)

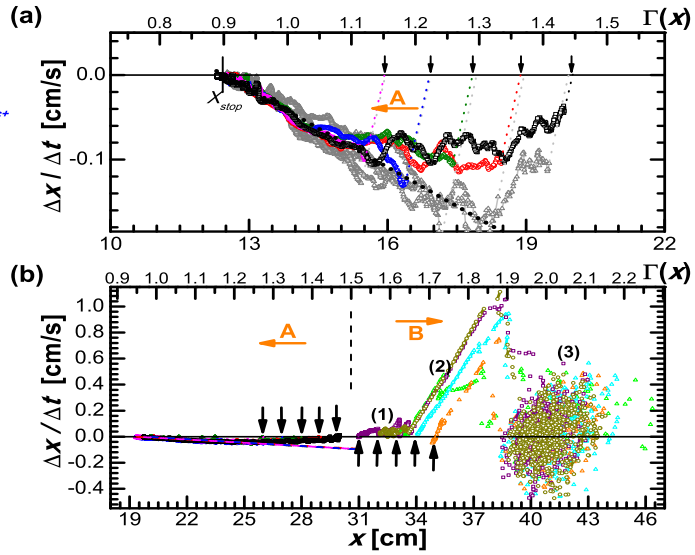

FIG. 3. The center-of-mass velocity of the chain plotted against its instantaneous position, with θ_0=0. **(a)** The crawling against the gradient exhibits a convergence regardless of the initial positions (indicated by vertical arrows). For a given driving condition (20Hz with VS=1.8), results from experiments with V-track (solid symbols) and with U-track (in light gray) show a similar profile. The dashed line represents the best linear fit, giving a well-defined stall position (X_{stop}). The velocity is computed at a time scale of Δt=4s with a sampling rate $1/dt$=8s^{-1}. **(b)** Observations made with a wider spatial range illustrate the vastly different magnitudes and spatial profiles for the two modes of ratcheting.(25Hz, VS=1.23, V-track; Δt=4s, $1/dt$=10s^{-1})

x for experiments with various tilt angle θ_0, all at the same driving condition. For the locations where Γ is well below unity, the chain exhibits no motion due to its inability to take off, just as one might expect. Once above this threshold, *within an appreciable range of* θ_0, our records demonstrate ratcheting movements with a spatial divide of directions: the chain either goes towards the decrease of vibration (scenario A) or in favour of the increase (scenario B). The steep change of the spatial range in which the chain exhibits uphill ratcheting against gravity defines a critical slope $\tan\theta_{c-}$. One may interpret this as an assessment of the "climbing force" in units of the weight of the chain. The determination of the upper critical slope $\tan\theta_{c+}$ may be somewhat uncertain due to the presence of the intervals exhibiting considerable fluctuations marked by brackets. Nevertheless, we have confirmed that the existence of these three different regimes is generic, and we collect in Fig. 2(b) the "phase boundaries" from data with different combinations of driving frequencies and strengths [11]. They look similar when plotted against Γ despite the values of VS varied by roughly a factor of three. Important information resides in the value $\tan\theta_{c-}$: the inset shows a plot against the gradient η evaluated at the location x_c where the uphill ratcheting last appears. This value appears insensitive to the driving frequency, but shows a strong correlation to VS and, in turn, the location x_c and the local gradient $\eta(x_c)$, as we will re-examine in later discussions.

We compute the velocity of the ratcheting chain along its trajectory and show in Figure 3. Panel (a) shows the slow crawling against the vibration gradient and that, for a fixed driving condition, the velocity (at a macroscopic timescale Δt) is insensitive to a considerable range of initial positions and appears as a function of x only. The velocity profiles measured with the two types of track appear similar. Panel (b) demonstrates the dramatic divide of the two directions of ratcheting and the vastly different magnitudes of speed between them. The development for a typical migration towards the direction of +x usually follows the sequence of (1) a developing stage with relatively slow migration , (2) a rapid acceleration, and (3) an apparently random final state (marked with brackets in Fig. 2a). In what follows, we look into

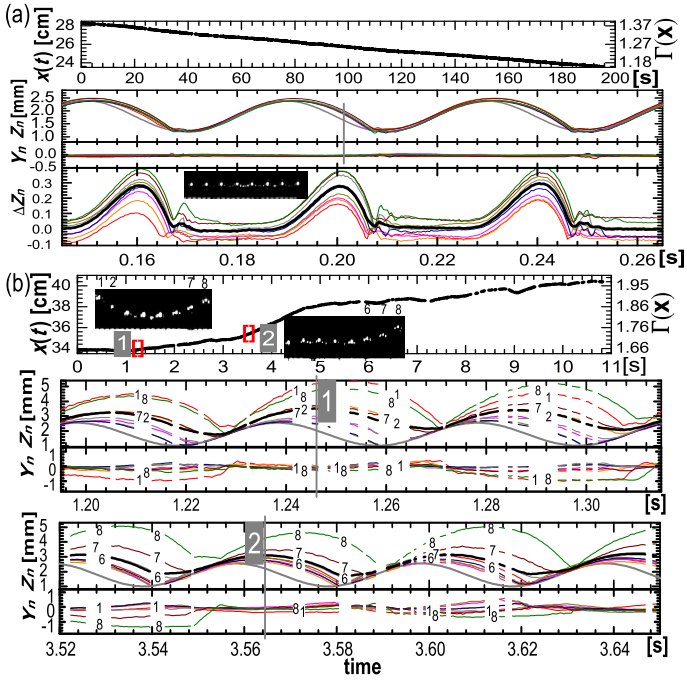

FIG. 4. High-speed 3D tracking of individual spheres (with the thick line representing their average, and the movement of the substrate plotted in gray), illustrating two qualitatively different modes of motion: **(a)** At a low excitation, the kinetic energy is nearly evenly distributed. The lowest panel magnifies the vertical motions with that of the substrate subtracted and shifted individually for clarity. **(b)** At a higher agitation, energy initially gather at the two free ends, then the right-hand side dominates and results in a dramatic acceleration towards +x. On the photos, only the indices of those spheres that are excited above the average are displayed. Both (a) and (b) are captured at a 25Hz-vibration with $\theta_0 = 0$ on V-track.

the multiple scenarios with further information obtained from high-speed three-dimensional (3D) imaging.

Figure 4 shows a typical data set obtained with our 3D particle tracking. The functions $Y_n(t)$ and $Z_n(t)$ show the time-resolved transverse coordinates of individual spheres as extracted from orthogonal imaging with two cameras synchronized at 2500frame/s. The projection of the center-of-mass of the chain on the x-axis is also determined by a third camera simultaneously from the top view at a much slower time scale. Fig. 4(a) illustrates the steady crawling (with the local excitation $\Gamma < 1.4$) in the direction of -x. All spheres follow the movements of the substrate for a considerable fraction of the oscillation period before they take off. Kinetic energy is largely dissipated upon the landing impacts well before their next departures, such that there is no obvious local accumulation of energy. In contrast, Fig. 4(b) shows a very different mode of motion, featuring a sequential developments: at its early stage (represented by snapshot 1, with its mean excitation $\Gamma \approx 1.66$), the accumulation of energy favours the two free ends which appear to "compete" with each other; this competition is then replaced with the dominance of the +x side (depicted as snapshot 2) with a prominent acceleration towards the right, before entering the unsteady final state (described as the "stage 3" in Fig. 3b). Time-resolved trajectories also illustrate the highly excited spheres making ballistic contacts with the substrate.

We believe that the three stages described above illustrate multiple developments of instability: the first transition occurs when Γ is strong enough to destabilise the relatively even distribution of energy (in reference to the periodic variation of potential energy as the chain follows the substrate, Fig. 4a); then the accumulation of energy near the two ends sets up a competition which makes the migration somewhat inefficient but still with a non-zero speed migrating towards +x presumably due to the vibration gradient; further increase of excitation as the chain advances may somehow make the competition unstable and replaced by the dominance of one end. It seems plausible to imagine that a swinging end would periodically pull the remaining part of the chain due to centrifugal force and result in the acceleration, although a thorough explanation requires further work. Nevertheless, one can be sure that which of the two free ends takes the lead would depend on the local asymmetry $\eta(x) \propto 1/x$, whose effect is expected to be compromised by stochastic fluctuations that grow with the excitation $\Gamma(x) \propto x$. One then would not be surprised that, as the chain moves further along +x, the development ends with the finale of back-and-forth movements when the two ends start to alternate their roles, because the dominance of the +x side can no longer be guaranteed once stochastic fluctuations override the local asymmetry.

For one who might wonder whether the slight oscillation of the normal vector $\hat{n}$ of the substrate could have been a factor that promotes ratcheting, we offer two reasons that should relieve this concern, both based on re-examining the measured values of critical slope (the inset of Fig. 2b): (a) the steady climbing towards -x does survive a considerable negative tilt with which $\hat{n}$ would always have a horizontal component towards +x, as the measured $|\tan\theta_{c-}|$ is well above the typical angular amplitude ($|\delta\hat{n}| \sim 0.002$ at 25Hz for VS=1); (b) keeping the same VS, the angular amplitudes for experiments at 15Hz and at 25Hz should have differed by about two times, but the measured $\tan\theta_{c-}$ is nearly unchanged. The evidence above, plus the strong correlation to VS and in particular $\eta(x_c)$, has convinced us that the observed steady crawling is mainly induced by the spatial asymmetry of vibration intensity.

One may also wonder whether a single particle alone could exhibit steady ratcheting in the presence of a vibration gradient. Instead of performing one-particle experiments that are practically impermissible due to the tendency to trigger continuous rolling, we assess its outcome by numerical simulations. To set the stage, we

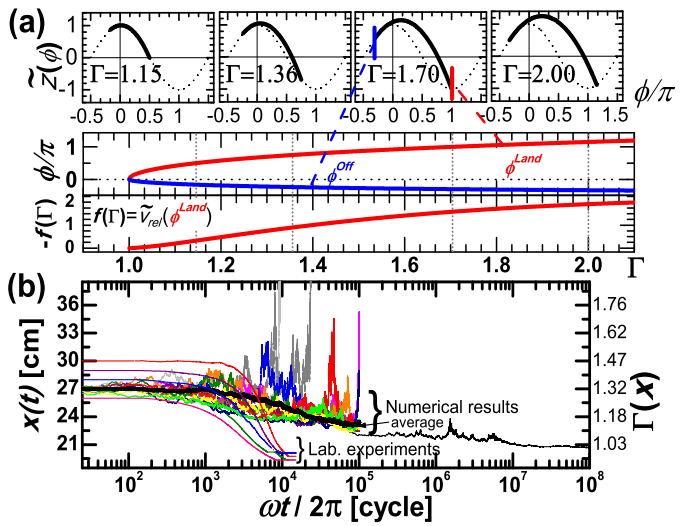

FIG. 5. **(a)** Local analyses of one particle taking off from an oscillating substrate at various values of Γ, and the impact speeds upon landing; **(b)** Simulations with a spatial gradient: the numerical results shown here include a random selection of twelve individual runs, the ensemble average over 74 runs (up to 10^5cycle), and one run up to 10^8 cycles, using a point-like particle with the same initial position $x(0) = 27$cm with $e = 0.5$. The data from laboratory experiments with five initial conditions (Fig. 3b, A) are also displayed here – note the relatively much smoother and faster motion of these ratcheting chains, compared to the numerical results.

analyse by elementary calculations the trajectory of a single particle that is initially at rest with the oscillating boundary and takes off as the acceleration of the boundary exceeds that of gravity. The results are presented in Fig.5(a), in which we assume a sinusoidal oscillation $(\Gamma g/\omega^2)\cos\omega t$ and use normalized coordinates $\phi \equiv \omega t$ and $\tilde{z} \equiv z/(\frac{\Gamma g}{\omega^2})$ such that the calculations are frequency-independent. The normalized velocity of impact upon landing, $\tilde{v}_{rel}$, is also numerically solved as a function $f(\Gamma)$. Then, for one particle bouncing on the substrate with a finite roughness and a spatial dependence $\Gamma(x)$, we assume that (a) the particle takes off from the substrate vertically, that (b) the landing impacts give the particle a horizontal momentum stochastically and allows the particle to move along x for a characteristic time δt before its energy is fully dissipated, and that (c) the time scale δt is smaller than the vibration period so that speed of the particle is reset to zero before the next cycle — in resemblance to the observed low-excitation scenario (Fig. 4a). We further quantify the horizontal momentum received upon landing as $(\hat{x}\cdot\vec{I}) \sim \epsilon_{xz}\, m v_{rel}\, \xi$, in which m is the particle mass, $v_{rel} = \tilde{v}_{rel}(\Gamma)\frac{\Gamma g}{\omega}$ is the impact velocity, ϵ_{xz} is a coupling constant reflecting the roughness, and ξ is a stochastic variable generated from a Gaussian distribution with a width of unity. The characteristic time of flight is estimated as $\delta t \sim 2e\, v_{rel}/g$ where e represents a restitution coefficient. Therefore, in every cycle the particle is expected to move by the distance $\delta x \sim \frac{1}{m}(\hat{x}\cdot\vec{I})\delta t = 2\epsilon|\Gamma f(\Gamma)|^2\xi\frac{g}{\omega^2}$, and the accumulation over a large number of vibrations would lead to the migration $x(t) = \int^t \delta x$, in which $\epsilon = \epsilon_{xz}e$.

With a vibration profile $\Gamma(x)$ matching one of the conditions in our laboratory experiments, sample results are shown in Fig. 5(b). Unlike the behaviours of actual granular chains in vibration gradients, the numerical results exhibit much higher fluctuations back and forth, because there is no way for these zero-dimension particles to explore the spatial asymmetry without randomly sampling the vibrations at different locations. A finite fraction of runs can even go temporarily off-chart (shown in light gray). The magnitudes of our numerical kicks are already at their theoretical upper limit as we set $e \sim O(1)$. Overall, the trajectories do exhibit a general trend of going towards -x, but their efficiency is in no comparison to that of the ratcheting motion in our laboratory experiments, in which chains moves more smoothly and much faster. In addition, we have extended our simulations to a linear chain by taking the approximation that N particles are constrained along x with a equal spacing, and we replace the horizontal impulse $(\hat{x}\cdot\vec{I})$ with $\Sigma_i^N(\hat{x}\cdot\vec{I}_i)$, the stochastic variable ξ with N-independent ones ξ_i, and the time scale δt with its value evaluated at the center of mass: our extended computations up to $N = 8$ do not show significant differences from the one-particle result, except with a slight reduction of the fluctuations [11]. Namely the simple summation over *uncorrelated* kicks received along a linear array in the thermal gradient is still inadequate to account for the observed steady crawling. These numerical experiments suggest that *cooperative* movements across the chain should have played important roles on the steady crawling towards -x as well, not just on the aforementioned rapid acceleration towards +x.

To summarize, by studying the responses of a granular chain in a non-uniform field of vibration, we have established that the spatial asymmetry of the intensity of vertical vibration can indeed induce sufficiently strong effect of ratcheting that often demands a considerable tilt of the substrate to counter balance. Two directions of ratcheting in relation to the vibration gradient are identified with qualitatively different modes of excitation. Time-resolved tracking of the chain motion provides us initial evidence of underlying transitions of granular dynamics and developing instabilities, for which further investigations are underway. Our numerical analyses start with a single stochastic particle and extend to summations over a linear array. The fact that the chain ratcheting observed in our laboratory experiments appear to be much "smarter" than the upper-bound predictions based on the thermophoresis-like picture indicates that delicate coordination along sub-units of the granular polymer should be a key factor behind their response to the spatial symmetry breaking.

ACKNOWLEDGEMENT

* Email address:

[1] S. Dorbolo, D. Volfson, L. Tsimring and A. Kudrolli, Phys. Rev. Lett. **95**, 044101 (2005)
[2] P. Brunet, J. Eggers and R. D. Deegan, Phys. Rev. Lett. **99**, 144501 (2007); K. John and U. Thiele, Phys. Rev. Lett. **104**, 107801 (2010).
[3] X. Noblin, R. Kofman and F. Celestini, Phys. Rev. Lett. **102**, 194504 (2009).
[4] Kiwing To, in preparation (2012).
[5] J.-C. Tsai, F. Ye, J. Rodriguez, J. P. Gollub and T. C. Lubensky, Phys. Rev. Lett. **94**, 214301 (2005).
[6] E. Ben-Naim, Z. A. Daya, P. Vorobieff and R. E. Ecke, Phys. Rev. Lett. **86**, 1414 (2001); Z. A. Daya, E. Ben-Naim and R. E. Ecke, Eur. Phys. J. E **21**, 1 (2006).
[7] Y.C. Chou, E. Cho, T.-H. Chou and T.M. Hong, Eur. Phys. J. E **29**, 157 (2009).
[8] K. Safford, Y. Kantor, M. Kardar and A. Kudrolli, Phys. Rev. E **79**, 061304 (2009)
[9] L.-N. Zou, X. Cheng, M. L. Rivers, H. M. Jaeger and S. R. Nagel, Science **326**, 408 (2009).
[10] E. Brown, A. Nasto, A. G. Athanassiadis and H. M. Jaeger, arXiv:1108.3315 [cond-mat] (2011).
[11] For the limited space here, the complete set of data plots and further details are provided on-line at http://www.phys.sinica.edu.tw/jctsai/chain-ratcheting/ and forthcoming as EPAPS-no-xxxxxxx